

Conference Paper

Misorientation Distribution Function of Crystals

Skrytnyy V. I., Gavrilov M. V., Khramtsova T. P., Kolyanova A. S., Krasnov A. S., Porechniy S. V., and Yaltsev V. N.

National Research Nuclear University MEPhI (Moscow Engineering Physics Institute), Kashirskoe shosse 31, Moscow, 115409, Russia

Annotation

When studying the structure of polycrystalline materials, the misorientation distribution function (MDF) is of great practical interest. In this paper we obtain preliminary calculated data on the MDF taking into account the position of the main maxima of the experimental orientation distribution functions (ODF) for recrystallized iron, rolled materials with a copper, silver, α -Fe, and brass texture, and also α -Zr based on direct pole figures of the rolled sample. It is shown that the proportion of brass rotations close to special is the largest, and amounts to 50%. The region of minimum rotations in the Euler space for cubic and hexagonal crystals is calculated.

Corresponding Author:

Valery Yaltsev

VNYaltsev@mephi.ru

Received: 21 December 2017

Accepted: 15 April 2018

Published: 6 May 2018

Publishing services provided by
Knowledge E

© Skrytnyy V. I. et al. This article is distributed under the terms of the [Creative Commons Attribution License](#), which permits unrestricted use and redistribution provided that the original author and source are credited.

Selection and Peer-review under the responsibility of the MIE-2017 Conference Committee.

1. Introduction

Most of the currently used industrial materials are polycrystalline, the properties of which are determined not only by grains, but also by grain boundaries [1]. The grain boundaries with orientational relationships that lead to the formation of coincident site lattices (CSL) have extreme properties associated with the grain boundary energy, grain boundary separations, migration of grain boundaries, slipping along grain boundaries, and so on. [2 - 4]. New materials with an increased content of such boundaries have improved properties, such as an increase in weldability by a factor of 50, a decrease in creep by a factor of 16, an increase in the service life by a factor of four [6] and an increase in the critical current by a factor of seven for high-temperature superconductors [7, 8]. In this connection, it is of interest to study methods for describing materials using the function of mutual rotations.

2. Materials and methods

The crystallographic texture, described by straight pole figures, inverse pole figures and the distribution function of orientations (DFO), characterizes the polycrystalline ensemble with respect to the chosen external coordinate system of the sample. To

 **OPEN ACCESS**

describe the orientation relationships between crystals, it is necessary to consider the (MDF). Since the mutual rotation of two grains can be specified by the rotation matrix **g** with the rotation angle α and the rotation axis **I** or the Euler angles ϕ, θ, ψ , the misorientations can be considered either in the crystallographic space the angle α -axis **I**, or in the Eulerian space.

If we express the components of the matrix **g** in terms of the angle α and the direction cosines of the rotation axis **I**, then the matrix **g** takes the form

$$g(l, \alpha) = \begin{vmatrix} l_1^2(1 - \cos\alpha) + \cos\alpha & l_1l_2(1 - \cos\alpha) - l_3\sin\alpha & l_1l_3(1 - \cos\alpha) + l_2\sin\alpha \\ l_1l_2(1 - \cos\alpha) + l_3\sin\alpha & l_2^2(1 - \cos\alpha) + \cos\alpha & l_2l_3(1 - \cos\alpha) - l_1\sin\alpha \\ l_1l_3(1 - \cos\alpha) - l_2\sin\alpha & l_2l_3(1 - \cos\alpha) + l_1\sin\alpha & l_3^2(1 - \cos\alpha) + \cos\alpha \end{vmatrix}$$

When using Euler angles ϕ, θ, ψ

$$g(\phi, \theta, \psi) = \begin{vmatrix} \cos\phi\cos\psi - \cos\theta\sin\phi\sin\psi & -\cos\phi\sin\psi - \cos\theta\sin\phi\cos\psi & \sin\theta\sin\phi \\ \sin\phi\cos\psi - \cos\theta\cos\phi\sin\psi & -\sin\phi\sin\psi + \cos\theta\cos\phi\cos\psi & -\sin\theta\cos\phi \\ \sin\theta\sin\psi & \sin\theta\cos\psi & \cos\theta \end{vmatrix}$$

Hamilton proposed a generalization of complex numbers $x + iy$ in the form of quaternions (from Latin quaterni - four), consisting of a real element and three imaginary units with real elements of the following form [9]: $\mathbf{R} = v_0 + v_1\mathbf{i}_1 + v_2\mathbf{i}_2 + v_3\mathbf{i}_3 = \text{scal}\mathbf{R} + \text{vect}\mathbf{R}$, where $\text{scal}\mathbf{R} = v_0$, $\text{vect}\mathbf{R} = v_1\mathbf{i}_1 + v_2\mathbf{i}_2 + v_3\mathbf{i}_3$.

When describing a rotation using an angle ϕ around axis with direction cosines l_1, l_2, l_3 of axis of rotation **I** and using Euler angles ϕ, θ, ψ quaternion components **R** have the form

$$\left. \begin{aligned} v_0 &= \cos\frac{\alpha}{2} = \cos\frac{\theta}{2}\cos\frac{\phi+\psi}{2} \\ v_1 &= l_1\sin\frac{\alpha}{2} = \sin\frac{\theta}{2}\cos\frac{\phi-\psi}{2} \\ v_2 &= l_2\sin\frac{\alpha}{2} = \sin\frac{\theta}{2}\sin\frac{\phi-\psi}{2} \\ v_3 &= l_3\sin\frac{\alpha}{2} = \cos\frac{\theta}{2}\sin\frac{\phi+\psi}{2} \end{aligned} \right\}$$

If two successive rotations are given by quaternions \mathbf{L} and \mathbf{M} , in that $\mathbf{L} = \lambda_0 + \lambda_1\mathbf{i}_1 + \lambda_2\mathbf{i}_2 + \lambda_3\mathbf{i}_3$ and $\mathbf{M} = \mu_0 + \mu_1\mathbf{i}_1 + \mu_2\mathbf{i}_2 + \mu_3\mathbf{i}_3$, then the resulting rotation $\mathbf{N} = \mathbf{LM}$ describes a quaternion $\mathbf{N} = v_0 + v_1\mathbf{i}_1 + v_2\mathbf{i}_2 + v_3\mathbf{i}_3$, where

$$v_0 = \lambda_0\mu_0 - \lambda_1\mu_1 - \lambda_2\mu_2 - \lambda_3\mu_3$$

$$v_1 = \lambda_0\mu_1 + \lambda_1\mu_0 + \lambda_2\mu_3 - \lambda_3\mu_2$$

$$v_2 = \lambda_0\mu_2 + \lambda_2\mu_0 + \lambda_3\mu_1 - \lambda_1\mu_3$$

$$v_3 = \lambda_0\mu_3 + \lambda_3\mu_0 + \lambda_1\mu_2 - \lambda_2\mu_1$$

Consequently, the misorientations of the crystals can be specified:

- by matrix $\mathbf{g}(\phi, \theta, \psi)$ with Euler angles ϕ, θ, ψ ;
- by matrix $\mathbf{g}(\phi_1, \phi_2, \phi_3)$ with angles of rotation ϕ_1, ϕ_2, ϕ_3 the axes of the selected Cartesian coordinate system;
- by matrix $\mathbf{g}(\alpha, \mathbf{l})$ with an angle of rotation α about the axis \mathbf{l} ;
- by quaternion.

Euler angles are often used in the theoretical analysis of the motion of a rigid body, the angles ϕ_1, ϕ_2, ϕ_3 – when the crystal is mounted on a goniometric head.

When studying the rotation of crystals, we are interested in the crystallographic indices of the axis of rotation and the value of the rotation angle, so in the future the parameters α and \mathbf{l} or ϕ_1, ϕ_2, ϕ_3 .

If any physical property is characterized by a function $\psi(r)$, then the theory of groups makes it possible to determine the influence of the symmetry of the coordinate (in the general case of a configuration space) on the properties of the function $\psi(r)$. In this case, because of the transformations \mathbf{R}_i physically equivalent functions appear $P_{R_i}\psi(r)$, where P_{R_i} – operator corresponding to \mathbf{R}_i .

By Wigner's rule $P_{R_i}\psi(R_i r) = \psi(r)$, or $P_{R_i}\psi(r) = \psi(R_i^{-1}r)$.

When examining a grain rotation as a function $\psi(r)$ acts as a rotation matrix \mathbf{A}_0 , so that matrices of equivalent rotations \mathbf{A}_i are determined as $A_i = A_0 R_i^{-1}$, where R_i^{-1} – elements inverse to elements \mathbf{R}_i of groups of pure rotations [10]. Each element of the group has one and only one inverse element, so if \mathbf{R}_i takes all the values of the elements of the group of pure rotations, then \mathbf{R}_i^{-1} also takes all the values of the elements of the same group, but in a different order. With considering $\mathbf{A}_j = \mathbf{A}_0 \mathbf{R}_j$, where \mathbf{R}_j – one of the elements of the corresponding group of pure rotations.

When calculating equivalent rotations in polycrystals, quaternions are preferred. Quaternions of elements of the group of pure rotations O and D_6 for cubic and hexagonal crystals are presented in Tables 1 and 2.

TABLE 1: Quaternions of elements of the group of pure rotations O of a cubic crystal.

Element of group	v_0	v_1	v_2	v_3	Element of group	v_0	v_1	v_2	v_3
E	1	0	0	0	$C_2^{[100]}$	0	1	0	0
$C_2^{[010]}$	0	0	1	0	$C_2^{[001]}$	0	0	0	1
$C_4^{[100]}$	$\frac{\sqrt{2}}{2}$	$\frac{\sqrt{2}}{2}$	0	0	$C_4^{[010]}$	$\frac{\sqrt{2}}{2}$	0	$\frac{\sqrt{2}}{2}$	0
$C_4^{[001]}$	$\frac{\sqrt{2}}{2}$	0	0	$\frac{\sqrt{2}}{2}$	$C_4^{[\bar{1}00]}$	$\frac{\sqrt{2}}{2}$	$-\frac{\sqrt{2}}{2}$	0	0
$C_4^{[0\bar{1}0]}$	$\frac{\sqrt{2}}{2}$	0	$-\frac{\sqrt{2}}{2}$	0	$C_4^{[00\bar{1}]}$	$\frac{\sqrt{2}}{2}$	0	0	$-\frac{\sqrt{2}}{2}$
$C_3^{[111]}$	$\frac{1}{2}$	$\frac{1}{2}$	$\frac{1}{2}$	$\frac{1}{2}$	$C_3^{[\bar{1}\bar{1}\bar{1}]}$	$\frac{1}{2}$	$-\frac{1}{2}$	$-\frac{1}{2}$	$-\frac{1}{2}$
$C_3^{[1\bar{1}\bar{1}]}$	$\frac{1}{2}$	$\frac{1}{2}$	$-\frac{1}{2}$	$\frac{1}{2}$	$C_3^{[\bar{1}\bar{1}1]}$	$\frac{1}{2}$	$-\frac{1}{2}$	$\frac{1}{2}$	$-\frac{1}{2}$
$C_3^{[11\bar{1}]}$	$\frac{1}{2}$	$\frac{1}{2}$	$\frac{1}{2}$	$-\frac{1}{2}$	$C_3^{[\bar{1}11]}$	$\frac{1}{2}$	$-\frac{1}{2}$	$-\frac{1}{2}$	$\frac{1}{2}$
$C_3^{[1\bar{1}1]}$	$\frac{1}{2}$	$\frac{1}{2}$	$-\frac{1}{2}$	$-\frac{1}{2}$	$C_3^{[111]}$	$\frac{1}{2}$	$-\frac{1}{2}$	$\frac{1}{2}$	$\frac{1}{2}$
$C_2^{[011]}$	0	0	$\frac{\sqrt{2}}{2}$	$\frac{\sqrt{2}}{2}$	$C_2^{[110]}$	0	$\frac{\sqrt{2}}{2}$	$\frac{\sqrt{2}}{2}$	0
$C_2^{[101]}$	0	$\frac{\sqrt{2}}{2}$	0	$\frac{\sqrt{2}}{2}$	$C_2^{[01\bar{1}]}$	0	0	$\frac{\sqrt{2}}{2}$	$-\frac{\sqrt{2}}{2}$
$C_2^{[1\bar{1}0]}$	0	$\frac{\sqrt{2}}{2}$	$-\frac{\sqrt{2}}{2}$	0	$C_2^{[10\bar{1}]}$	0	$\frac{\sqrt{2}}{2}$	0	$-\frac{\sqrt{2}}{2}$

For a polycrystal, the set of all possible misorientation angles is a ball of radius π . The rotation in this case is determined by a vector of length α along the axis \mathbf{l} , given by angles θ and φ . To determine the distribution density of the rotation angles $P(\alpha)$, it is necessary to perform invariant integration [9, 11] with respect to the parameters θ and φ , which determines the position of the rotation axes, within the volume of the region of minimum rotations:

$$P(\alpha) = \frac{(1 - \cos \alpha) \int_{V_E} \sin \theta d\theta d\varphi}{4\pi^2}.$$

This integration corresponds to calculating the cross-sectional area of the region V_E of minimal rotations by a sphere of radius α .

TABLE 2: Quaternions of elements of the pure rotation group D_6 of the hexagonal crystal.

Element of group	v_0	v_1	v_2	v_3	Element of group	v_0	v_1	v_2	v_3
E	1	0	0	0	$C_2^{[\bar{1}2\bar{1}0]}$	0	$-\frac{1}{2}$	$\frac{\sqrt{3}}{2}$	0
$C_2^{[2\bar{1}\bar{1}0]}$	0	1	0	0	$C_2^{[\bar{1}100]}$	0	$-\frac{\sqrt{3}}{2}$	$\frac{1}{2}$	0
$C_2^{[01\bar{1}0]}$	0	0	1	0	$C_3^{[0001]}$	$\frac{1}{2}$	0	0	$\frac{\sqrt{3}}{2}$
$C_2^{[0001]}$	0	0	0	1	$C_3^{[000\bar{1}]}$	$\frac{1}{2}$	0	0	$-\frac{\sqrt{3}}{2}$
$C_2^{[10\bar{1}0]}$	0	$\frac{\sqrt{3}}{2}$	$\frac{1}{2}$	0	$C_6^{[0001]}$	$\frac{\sqrt{3}}{2}$	0	0	$\frac{1}{2}$
$C_2^{[\bar{1}120]}$	0	$-\frac{1}{2}$	$-\frac{\sqrt{3}}{2}$	0	$C_6^{[000\bar{1}]}$	$\frac{\sqrt{3}}{2}$	0	0	$-\frac{1}{2}$

Fig. 1-3 shows the distribution density of the misorientations $P(\alpha)$ for cubic and hexagonal crystals.

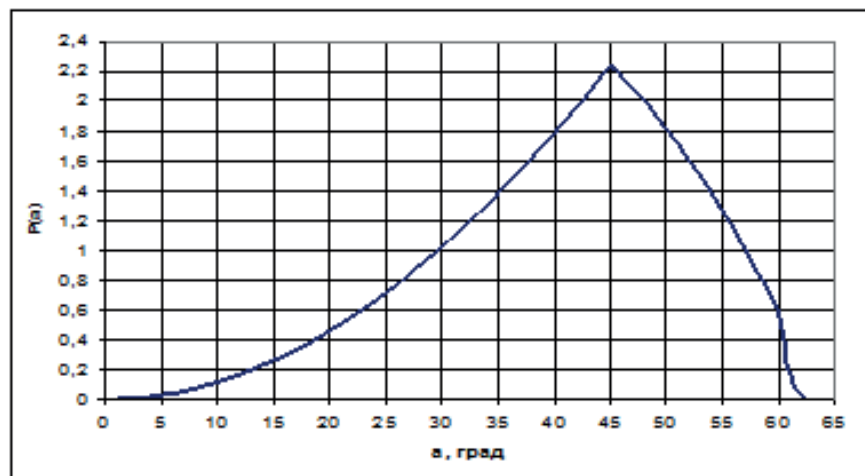


Figure 1: The density distribution of the misorientation angles $P(\alpha)$ for cubic crystals.

For certain rotation parameters, there are coincidence lattices, and if the boundary coincides with the most densely packed plane of the coincidence lattice, then the energy of the boundary is minimal.

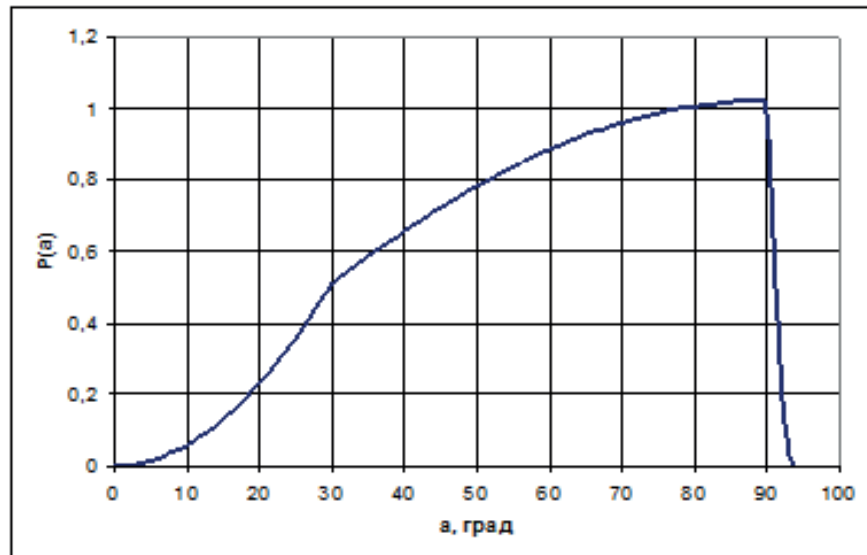


Figure 2: The density distribution of the misorientation angles $P(\alpha)$ for hexagonal crystals.

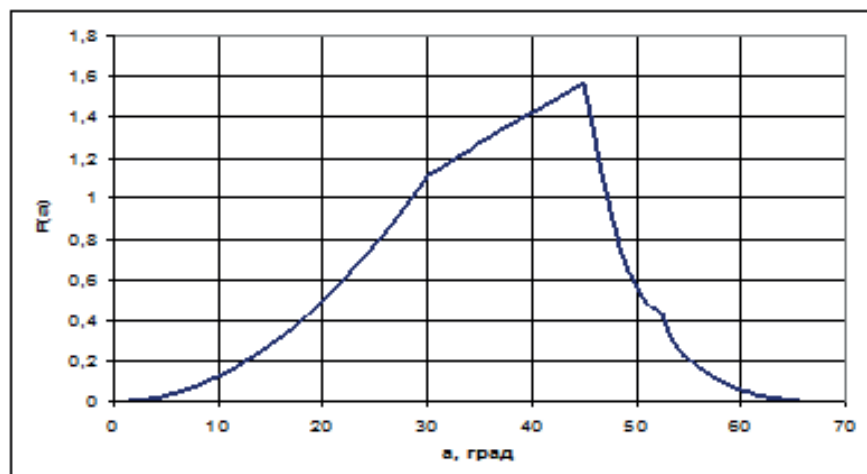


Figure 3: The density distribution of the misorientation angles $P(\alpha)$ for cubic and hexagonal crystals.

Special properties of the grain boundaries are preserved for small deviations of the misorientations of neighboring grains from a special one. The maximum deviation angle (in radians) from a special orientation, when accommodation with grain boundary dislocations is still possible and special properties are retained, is defined as

$$\Delta\alpha = \frac{10 \div 15}{\pi\sqrt{\Sigma}}$$

Fig. 4 shows in the standard triangle the misorientations of the cubic lattices creating the CSL with $\Sigma < 150$.

Fig. 5-6 shows the distribution of the rotations corresponding to the appearance of coincident site lattices for cubic and hexagonal crystals.

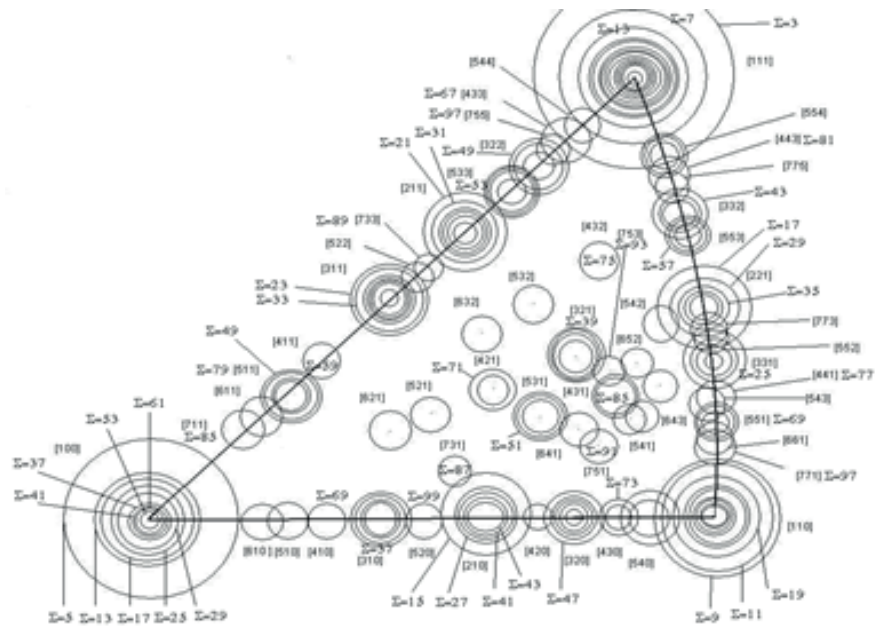


Figure 4: Distribution of misorientations corresponding to emergence of coincidence site lattices with $\Sigma < 150$, for cubic crystals.

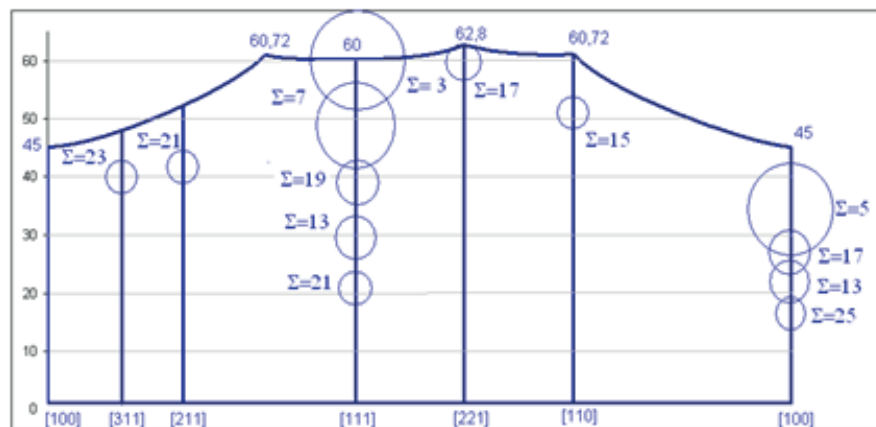


Figure 5: Distribution of misorientations corresponding to emergence of coincidence site lattices to $\Sigma = 25$ for cubic crystals on the sides of the standard stereographic triangle.

3. Results

Preliminary calculated data on the MDF taking into account the position of the main maxima of experimental orientation distribution functions (Fig. 7) for rolled materials with a copper-type texture (Fig. 8), silver (Fig. 9), α -Fe (Fig. 10) and brass (Fig. 11). On the charts rotation axis – the minimum rotation angle, the positions of the special rotations with $\Sigma \leq 25$ are also shown.

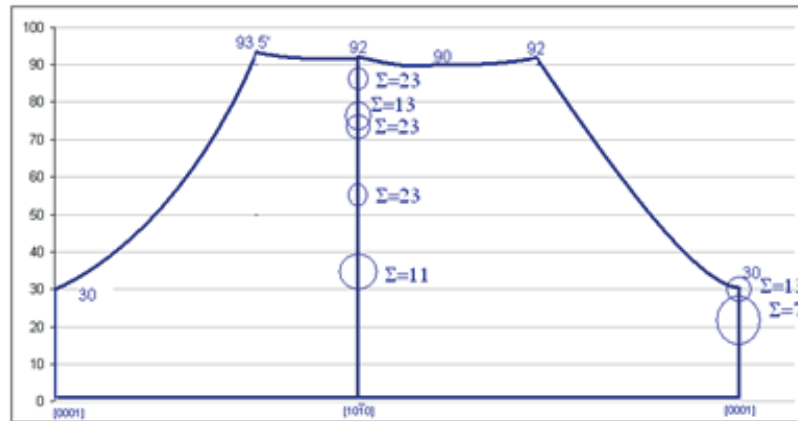


Figure 6: Distribution of misorientations corresponding to emergence of coincidence site lattices to $\Sigma = 23$ for hexagonal crystals on the sides of the standard stereographic triangle.

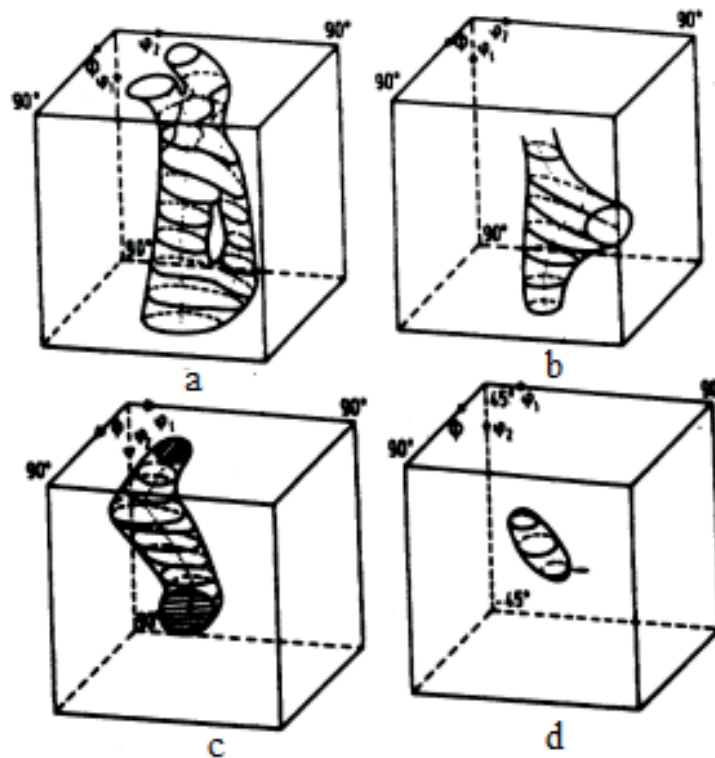


Figure 7: Orientation distribution functions for different types of textures: a) recrystallized iron, b) rolled iron, c) rolled copper, d) rolled brass.

MDF can be represented in space by the axis of the turn in the stereographic triangle - the minimum rotation angle.

Fig. 12 - 13 presents preliminary data on ODF for α -Zr on the basis of analysis of the pole figures of the rolled α -Zr sample.

In texture analysis, the orientation distribution function is usually considered in Eulerian space with angles φ , θ , ψ varying in the interval $0 - \pi/2$. When using the MDF

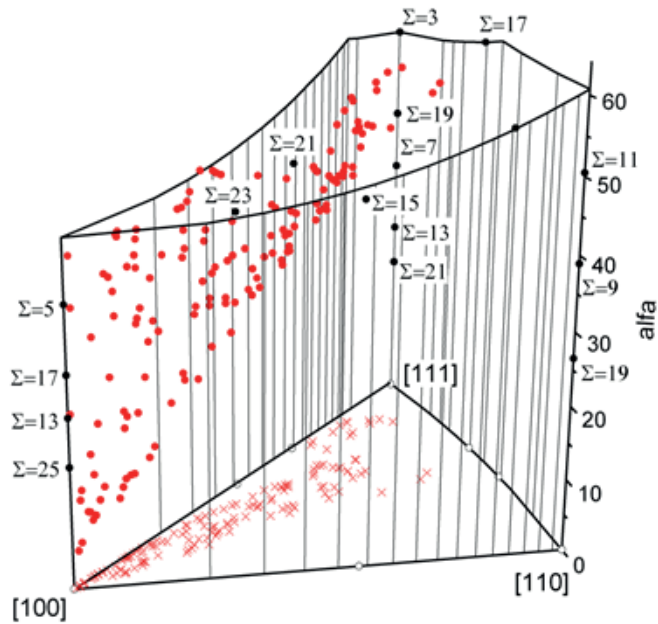


Figure 8: Distribution of misorientations in the angle-axis space for Cu rolling texture (● – rotations of Cu crystals and × – their projections, ● – special rotations and ° – their projections).

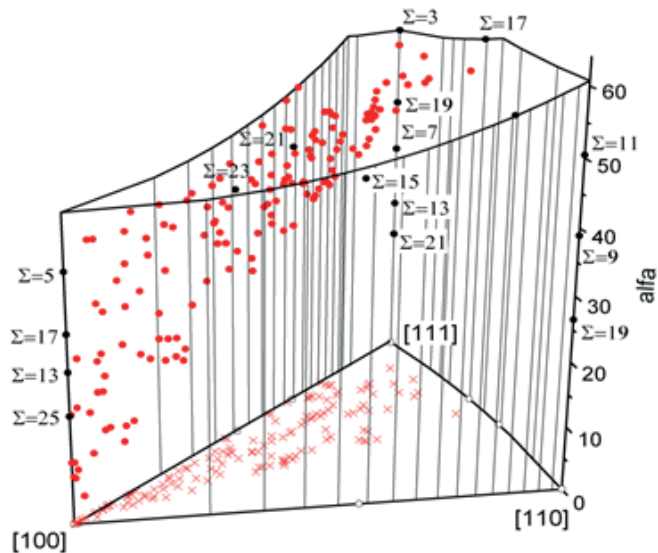


Figure 9: Distribution of misorientations in the angle-axis space for Ag rolling texture (● – rotations of Ag crystals and × – their projections, ● – special rotations and ° – their projections).

in Euler space, it is desirable to determine the region corresponding to the minimum misorientation angles.

For cubic crystals, a region with Euler angles φ, θ, ψ varying in the interval $0 - \pi/2$ is basically determined by an equivalent rotation due to the symmetry element C_{4-x} and for hexagonal crystals by symmetry elements $C_6^{[0001]}$ and $C_3^{[0001]}$ (Fig. 14).

The regions of the Eulerian space corresponding to the minimum misorientation angles for cubic and hexagonal crystals are shown in Fig. 15, 16.

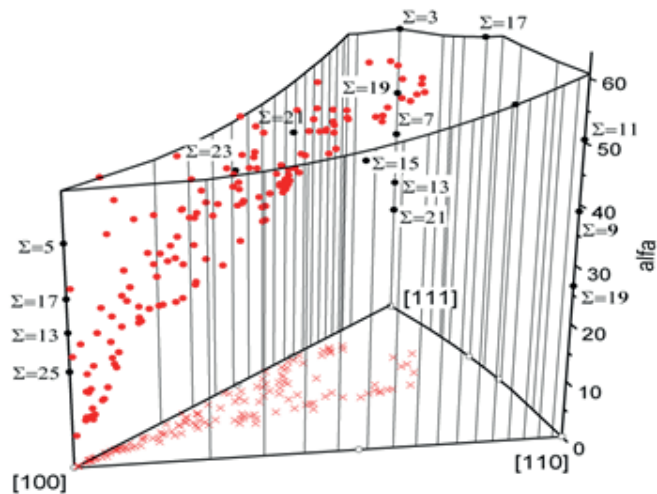


Figure 10: Distribution of misorientations in the angle-axis space for α -Fe rolling texture (● – rotations of α -Fe crystals and × – their projections, ● – special rotations and ° – their projections).

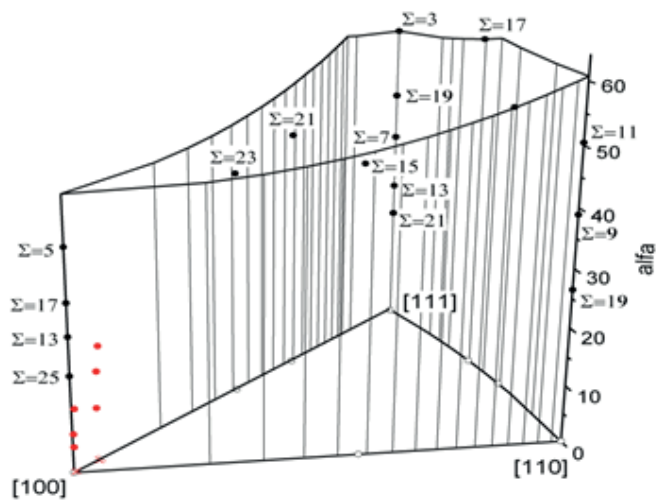


Figure 11: Distribution of misorientations in the angle-axis space for brass rolling texture (● – rotations of brass crystals and × – their projections, ● – special rotations and ° – their projections).

4. Discussion

The nature of the distribution of misorientations in the Eulerian space for these materials is quite similar: the rotations are located mainly in a certain part of the volume - the most uniform distribution is observed in α -Fe, the remaining materials exhibit areas of increased concentration of rotations. The arrangement of small-angle rotations ($\alpha < 15^\circ$) is analogous for all materials near the [100] axis in a small region corresponding to $\Sigma = 5$.

Some differences in the distribution of the rotations are observed when they are represented in the space by the angle-axis of the rotation, while the rotations occupy

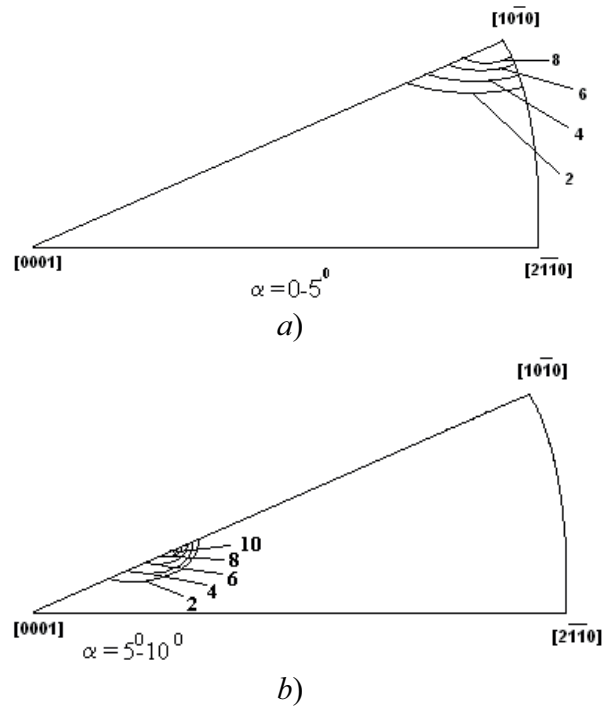


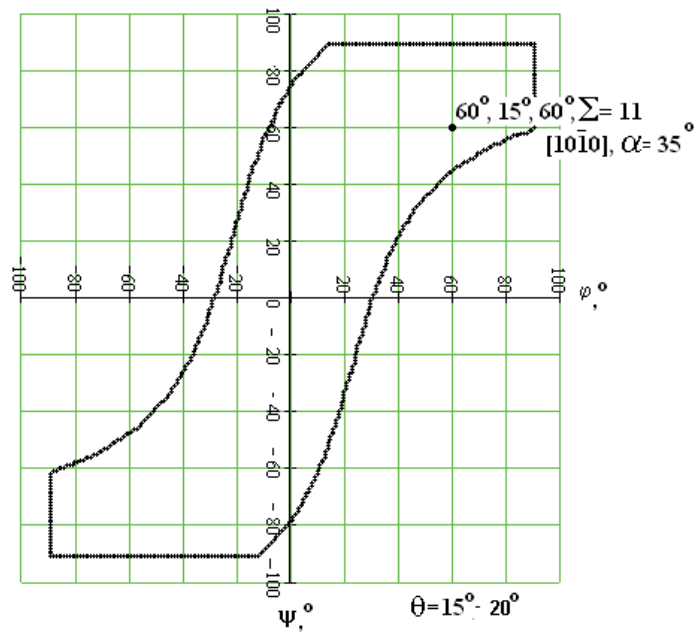
Figure 12: Mutual rotation function for rolled α -Zr in space angle α -axis / for cross sections α a) $0^\circ - 5^\circ$; b) $5^\circ - 10^\circ$.

not the entire region of the stereographic projection but are located closer to its boundary $[100] - [111]$. The greatest concentration of rotations near $\Sigma = 5$ is observed in α -Fe. Silver rotations are the most uniform distribution in the whole area of their location. In the copper rotations, ignoring of special rotations with $\Sigma = 21, 23$ is observed, and it is clearly visible that there are no rotations around the axes of these boundaries.

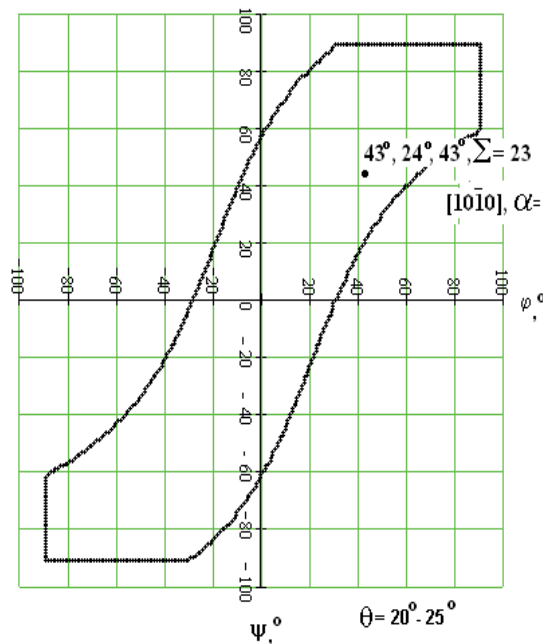
The angles of misorientations for brass are located closer to the rotations corresponding to the occurrence of coincidence grids. The share of misorientations close to special ones: Cu - 20%, Ag - 30%, α -Fe - 24%, brass - 50%.

The region of the minimum angles of equivalent turns in a cubic crystal in the region of Euler angles φ, θ, ψ varying in the interval $0 - \pi/2$ has the form of a hexagonal prism with a base in the plane $\theta = 0^\circ$, height $\theta = 45^\circ$, with a pyramidal peak. The edges of this prism correspond to the edges of this region and to the planes $\varphi - \psi = 45^\circ$ and $\varphi - \psi = -45^\circ$. The maximum of the pyramidal peak is at the center of this region of the Eulerian space, and corresponds to $\theta = 60^\circ$. For hexagonal crystals, the region of minimum angles is in the form of three hexagonal prisms with flat tops, a height $\theta = 90^\circ$.

In the region of Euler angles φ and ψ from $-\pi/2$ to $+\pi/2$, a similar picture is observed. Both for cubic and hexagonal crystals in the region of negative φ and ψ there is a copy



a)



b)

Figure 13: The misorientation distribution function for rolled α -Zr in the Eulerian space a) $\theta 15^\circ - 20^\circ$; b) $\theta 20^\circ - 25^\circ$.

of the prism from the positive region. However, there is one peculiarity, namely, the existence of a slope plane in the region of negative ψ , whose base line goes from the point $\varphi = 30^\circ, \psi = 0^\circ$ to the point $\varphi = 0^\circ, \psi = -90^\circ$ and increases in the direction of ψ and decreasing φ . The reason for its occurrence is probably the singularity of the Eulerian

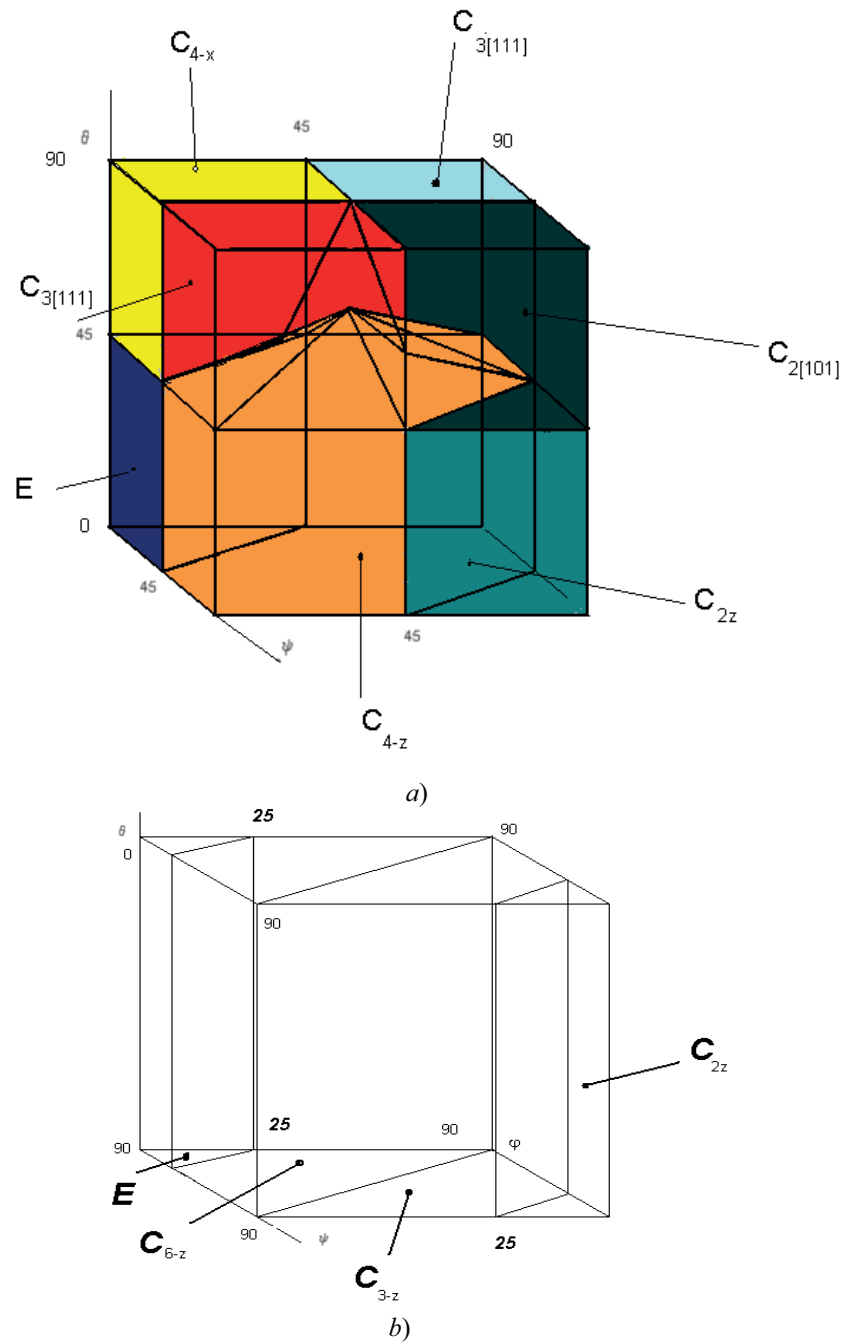
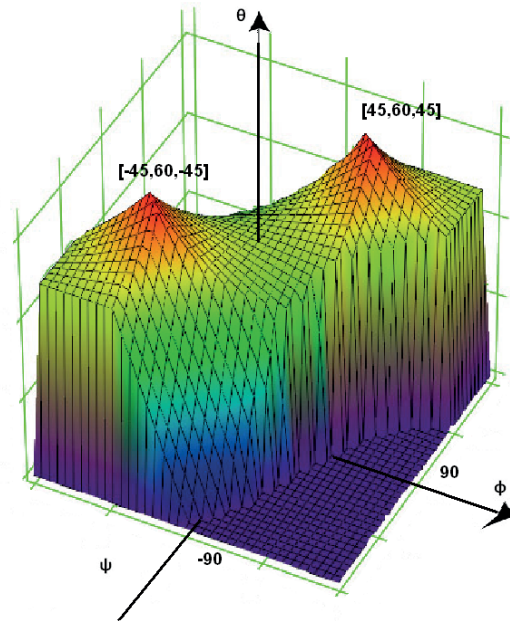


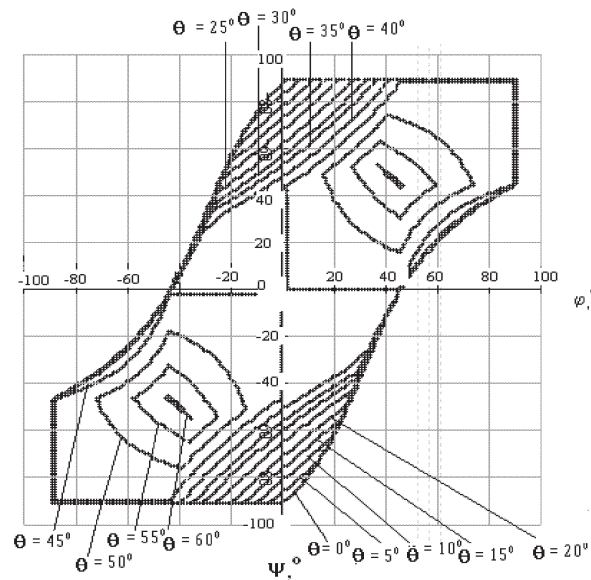
Figure 14: The regions of minimum angles of equivalent rotations in the orientation space for cubic (a) and hexagonal crystals (b).

space, in which the angles φ and ψ for small values of θ correspond to rotations around close to each other axes.

It is interesting to note that there is a certain similarity between the graph of the distribution density of the misorientation angles $P(\alpha)$ and the form of the regions of minimal angles of equivalent rotations. Thus, the position of the maximum of the



a)



b)

Figure 15: a) The region of the minimum rotation angles for cubic crystals in the Eulerian space (half is shown corresponding to the positive values of θ); b) cross-sections of the region of the minimum angles of rotation at angles θ for cubic crystals in the Eulerian space.

angular distribution density coincides in magnitude with the height of the prism in the Eulerian space for both cubic and hexagonal crystals.

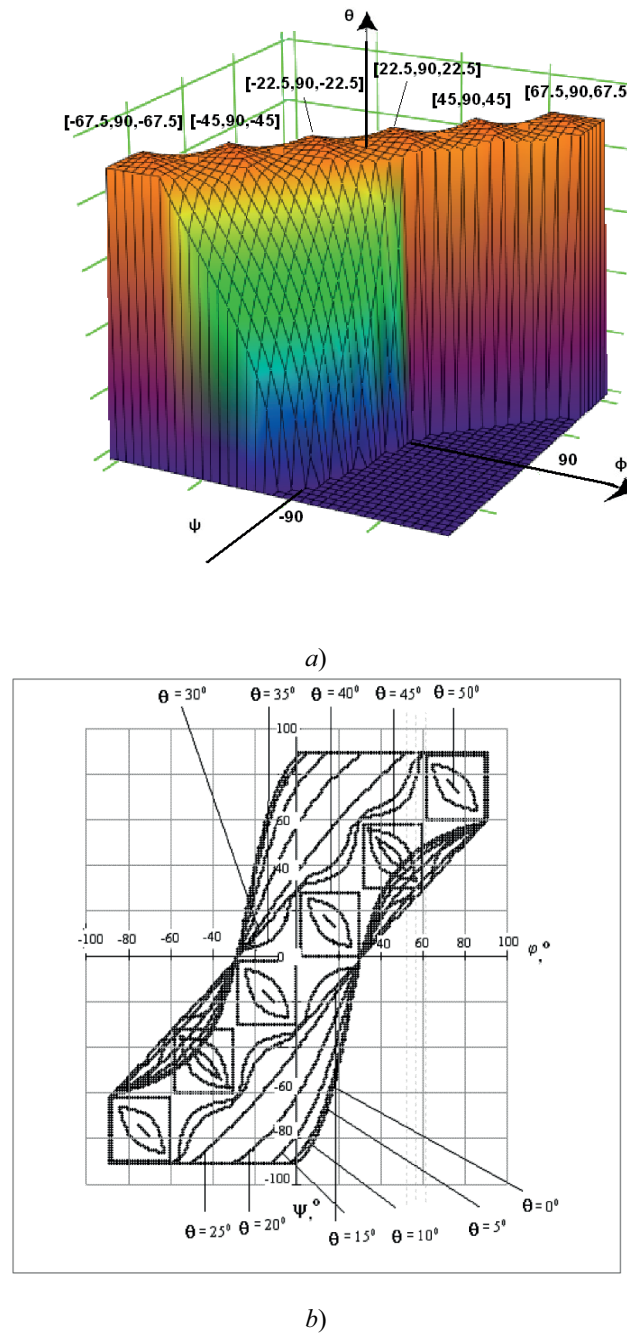


Figure 16: a) The region of the minimum rotation angles for hexagonal crystals in the Eulerian space (half is shown corresponding to the positive values of θ); b) cross-sections of the region of the minimum angles of rotation at angles θ for hexagonal crystals in the Eulerian space.

5. Conclusion

In this paper we obtain preliminary calculated data on the MDF taking into account the position of the main maxima of the experimental orientational distribution functions for recrystallized iron, rolled materials with a copper, silver, α -Fe, and brass texture, and also α -Zr based on direct pole figures of the rolled α -Zr sample. The region of

minimum rotations in the Euler space for cubic and hexagonal crystals is calculated. The results obtained can be used in further studies.

References

- [1] Kaibyshev O.A., Valiev R.Z., Boundaries of grains and properties of metals, Moscow, Metallurgiya, 1987, 214 p.
- [2] Gleiter G., Chalmers B., Large-angle grain boundaries, Moscow, Mir, 1975, 376 p.
- [3] Gleiter H., Chalmers B., High-angle grain boundaries, Progress in materials science, 1972, 593 – 602 p.
- [4] Patale S., Mason J. K., Schon C., Improved representation information for grain boundary science and engineering, Progress in material science, 57, (2012), p.1383.
- [5] Lehockey E. M., Palumbo G., On the creep behaviour of grain boundary engineered nickel, Materials Science and Engineering: A., 237,(1997), p. 168 - 172.
- [6] Lehockey E. M., Palumbo G., Lin P., On the relationship between grain boundary character distribution and intergranular corrosion, Scripta Materialia, 36, (1997), p. 1211 - 1218.
- [7] David P. Norton et al, Formation of artificially-layered high-temperature superconductors using pulsed-laser deposition, Applied Surface Science, 98, (1996), p. 672 - 678.
- [8] Weijiu Huang et al., Evolution of microstructure and grain boundary character distribution of a tin bronze annealed at different temperatures, Materials Characterization, 114, (2016), p. 204 - 210.
- [9] Branets V.N., Shmyglevsky I.P., Application of quaternions in problems of orientation of a rigid body, Nauka Publishers, Moscow, 1973, 320 p.
- [10] Khamermesh M., Theory of groups and its application to physical problems, Moscow, Editorial URSS, 2002, 587 p.
- [11] MacKenzie J. K., The distribution of rotation axes in a random aggregate of cubic crystals, Acta Metall, 1964, 12, 223–225 p.